

# A study of X-ray luminescence and spectral compatibility of europium-activated yttrium-vanadate ( $\text{YVO}_4:\text{Eu}$ ) screens for medical imaging applications

G. Panayiotakis<sup>1</sup>, D. Cavouras<sup>2,\*</sup>, I. Kandarakis<sup>2</sup>, C. Nomicos<sup>3</sup>

<sup>1</sup> Department of Medical Physics, Medical School, University of Patras, GR-265 00 Patras, Greece

<sup>2</sup> Department of Medical Instrumentation Technology, Technological Educational Institution of Athens, 37-39 Esperidon Street, GR-17671 Athens, Greece  
(Fax: + 30-1/5910-975)

<sup>3</sup> Department of Physics, Technological Educational Institution of Piraeus, Thivon, Aigaleo, Greece

Received: 24 July 1995/Accepted: 14 November 1995

**Abstract.** The X-ray luminescence efficiency of laboratory-prepared  $\text{YVO}_4:\text{Eu}$  screens and their spectral compatibility to common optical detectors were studied under medical fluoroscopy conditions.  $\text{YVO}_4:\text{Eu}$  screens were prepared by sedimentation and with different coating thickness. Luminescence efficiency of the  $\text{YVO}_4:\text{Eu}$  screens was measured at various X-ray tube voltages (50–250 kVp) and for screens of different coating thicknesses (20–180 mg/cm<sup>2</sup>). Spectral response was also measured and spectral matching factors between the  $\text{YVO}_4:\text{Eu}$  screens and some common optical detectors (photocathodes, photodiodes, photographic emulsion) were calculated. Experimental results on efficiency were fitted by formulas of the theoretical model developed by Hamaker and Ludwig in order to determine phosphor intrinsic X-ray-to-light conversion efficiency and intrinsic optical characteristics, such as coefficients related to light scattering and absorption. Although the luminescence efficiency of  $\text{YVO}_4:\text{Eu}$  screens was found to be relatively low (3–11  $\mu\text{W s/mR m}^2$ ), the matching factor of  $\text{YVO}_4:\text{Eu}$  screens with some red sensitive optical detectors was excellent, of the order of 0.96. High spectral compatibility may indicate that  $\text{YVO}_4:\text{Eu}$  scintillators could be used in medical image detectors.

**PACS:** 78.65; 42.80

Fluorescent materials coupled to optical photon detectors (e.g. photographic emulsion, photocathode, photodiode) have been used in a vast number of applications in medical imaging. The luminescence of these materials and the spectral compatibility between light emitted and spectral sensitivity of the optical photon detector are important factors in the design of radiation detectors of medical imaging systems.

\*To whom all correspondence should be addressed

Terbium activated rare-earth materials emitting bluish–greenish light have been widely studied [1–3] but, to our knowledge, there has been only one report [4] on europium activated scintillators ( $\text{Y}_2\text{O}_2\text{S}:\text{Eu}$ ) emitting reddish light under medical fluoroscopy conditions. Europium activated yttrium vanadate ( $\text{YVO}_4:\text{Eu}$ ) is a red light emitting scintillator that has been previously used in color television for both color and brightness improvement as well as in luminescent and mercury-vapor lamps for color–rendering improvement [5]. Since the light spectrum of  $\text{YVO}_4:\text{Eu}$  [5] seems to match the spectral sensitivity of some optical photon detectors, often used in medical imaging (e.g. red sensitive films, photodiodes, photocathodes), a study of  $\text{YVO}_4:\text{Eu}$  luminescence, spectral response, and compatibility under excitation by X-rays from medical X-ray tubes was performed. Luminescence was assessed by determining the ratio of the light flux emitted from the phosphor screen to the exposure rate of X-rays incident on the screen for various tube voltages and coating thickness; this ratio constitutes the absolute efficiency of the screen [6]. Spectral response of  $\text{YVO}_4:\text{Eu}$  was measured and its spectral compatibility with known optical photon detectors was determined by calculating the corresponding spectral matching factors.

## 1 Material and methods

The experimental set up used for luminescence measurements comprised a radiotherapy X-ray unit (Siemens Stabilipan), a photomultiplier tube with an extended S-20 photocathode, a Cary 401 vibrating reed electrometer, a PTW dosimeter for exposure rate measurements and an Oriel 7240 grating monochromator for light spectrum determination. A detailed description is given in previous papers [3, 4].

The phosphor material was supplied in powder form by Derby Luminescents Ltd. (Code No.1510). Fluorescent layers (screens) were prepared by a sedimentation technique on fused silica substrates from a mixture consisting of 2.0 l of deionized water, 25 ml  $\text{Na}_2\text{SiO}_3$  aqueous solution (refraction index 1.353).  $\text{Na}_2\text{SiO}_3$  is acting as binder

material between phosphor grains. The amount of fluorescent material varied from 1 to 20 g depending on the screen coating thickness, which ranged between 20 and 180 mg/cm<sup>2</sup>.

Two modes of light flux measurement were followed: (a) transmission observation mode, for light emitted from the screen surface opposing that of the X-ray beam incidence, and (b) reflection observation mode, for light emitted by the surface receiving the X-rays. The first mode corresponds to most cases of scintillator-optical detector configurations (image intensifiers, computed tomography, computed radiography and nuclear medicine detectors, front screen radiographic cassettes). The second mode corresponds to the special case of rear intensifying screens used in double coated radiographic cassettes or in single coated mammographic screens. Experimental data were obtained over a wide range of X-ray tube voltages from 50 to 250 kVp with tube current setting at 10 mA.

Hamaker [7] and Ludwig [6] have theoretically formulated the problem of luminescence induced by monochromatic X-rays in an homogeneous fluorescent slab sandwiched between two substrates. Light creation and penetration within the screen material is described by the following differential equations:

$$\frac{dI_F}{dW} = -(a + s) \cdot I_F + s \cdot I_B + \frac{1}{2} n_c \cdot \mu \cdot N \cdot e^{[-\mu W]}, \quad (1)$$

$$\frac{dI_B}{dW} = (a + s) \cdot I_B - s \cdot I_F - \frac{1}{2} n_c \cdot \mu \cdot N \cdot e^{[-\mu W]}, \quad (2)$$

where  $I_F$ ,  $I_B$  are forward and backward, relative to X-ray incidence, light intensities,  $a$  and  $s$  are the light absorption and light scattering coefficients,  $\mu$  is the X-ray mass attenuation coefficient,  $n_c$  is the intrinsic X-ray to light conversion efficiency of the fluorescent material,  $N$  is the X-ray beam power,  $W$  is the screen coating thickness. The solution of the above equations gives absolute efficiency as a function of optical parameters  $n_c$ ,  $\beta$ ,  $\sigma$  and coefficient  $\mu$  (see appendix):

$$n_T(E) = f(n_c, \beta, \sigma, \mu), \quad (3)$$

$$n_R(E) = f(n_c, \beta, \sigma, \mu), \quad (4)$$

where,  $n_T(E)$ ,  $n_R(E)$  are the monochromatic absolute efficiencies in transmission and reflection observation mode, respectively, and  $\sigma$  and  $\beta$  are coefficients related to light scattering ( $s$ ) and absorption ( $a$ ) as follows:

$$\sigma = [a(a + 2s)]^{1/2}, \quad (5)$$

$$\beta = \left[ \frac{a}{a + 2s} \right]^{1/2}. \quad (6)$$

The expectation value of absolute efficiency over the whole X-ray energy spectrum (polychromatic efficiency) was obtained using relation (7):

$$n_0 = \frac{\int_0^{E_0} n_i \cdot f(E) \cdot dE}{\int_0^{E_0} f(E) \cdot dE}, \quad (7)$$

where  $i = T$  or  $R$  are for transmission and reflection, respectively, and  $f(E)$  is the X-ray source spectral response

function given by Storm [8]:

$$f(E) = \left( 1 - \frac{E}{E_0} \right) \cdot e^{(-\mu_{Al} \cdot d)} \quad (8)$$

where  $\mu_{Al}$  is the X-ray attenuation coefficient for aluminum and  $d$  is the aluminum thickness (2 mm tube filter and 20 mm filter simulating X-ray attenuation by human tissues). X-ray attenuation coefficients introduced in the model formulas (3) and (4) were calculated from data on yttrium, vanadium, and oxygen given by Storm and Israel [9] and Saloman et al. [10]. Coefficient  $\sigma$  and intrinsic efficiency  $n_c$  were determined by fitting the theoretical formulas (3) and (4) to experimental data. Coefficient  $\beta$  was calculated from reflectivity measurements according to Ludwig [6].

Spectral compatibility was assessed by calculating the matching factor [11] between the  $YVO_4:Eu$  light spectrum and the spectral sensitivity distribution of several commonly used optical detectors. The matching factor  $a_s$  was determined by means of relation (9):

$$a_s = \frac{\int_{\lambda_1}^{\lambda_2} F_s(\lambda) S(\lambda) d\lambda}{\int_{\lambda_1}^{\lambda_2} F_s(\lambda) d\lambda}, \quad (9)$$

where  $F_s(\lambda)$  is the normalized spectral distribution of the emitted light,  $S(\lambda)$  is the normalized distribution function of the optical detector's spectral sensitivity.  $\lambda_1$ ,  $\lambda_2$  are the lower (575 nm) and upper (680 nm) limits of the light spectrum.  $YVO_4:Eu$  light spectrum was measured by means of the monochromator and spectral compatibility of  $YVO_4:Eu$  was studied with the following detector materials; GaAs, GaAsP, extended GaAsP, S-20, extended S-20, modified S-20, S-25, Si, Ge, and Agfa Scopix LT 2B photographic emulsion. Spectral sensitivity distributions were made available by EMI, RCA, Hamamatsu, ITL, Rofin, and Agfa manufacturers. Since experimental data on absolute efficiency of  $YVO_4:Eu$  screens were obtained by the extended S-20 photocathode, the corresponding matching factor was taken into account for absolute efficiency data correction.

## 2 Results and discussion

Figures 1 and 2 show the variation of absolute efficiency with tube voltage for three different thickness screens (21, 58, 135 mg/cm<sup>2</sup>) measured both in transmission and reflection mode observation, respectively; peak values of efficiency appear in the 70–90 kVp range, which is within the useful kVp range used in diagnostic radiology. In Fig. 3, the peak absolute efficiency of all the  $YVO_4:Eu$  screens studied against their coating thickness in transmission and reflection mode is presented. Reflection mode efficiency is increasing towards a saturation value while transmission mode efficiency shows a peak value around 140 mg/cm<sup>2</sup>. As shown in Figs 1–3 transmission mode efficiency was lower than reflection mode efficiency, especially in the useful radiographic range (50–100 kVp) of tube voltages and for all screen thicknesses; this was expected considering the additional grain layers, that light

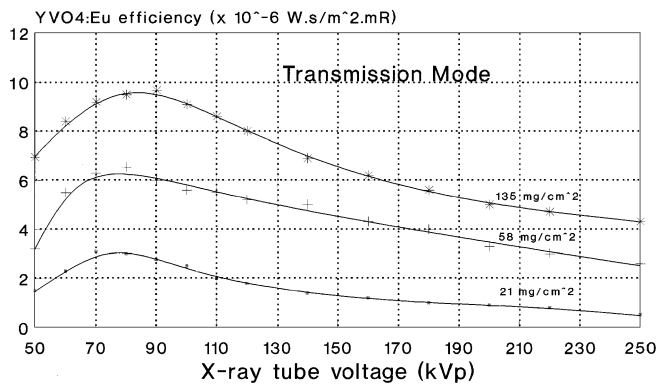


**Fig. 1.** Absolute efficiency of three  $\text{YVO}_4:\text{Eu}$  screens against X-ray tube voltage in transmission mode observation. *Points*: experimental data; *solid lines*: theoretical results

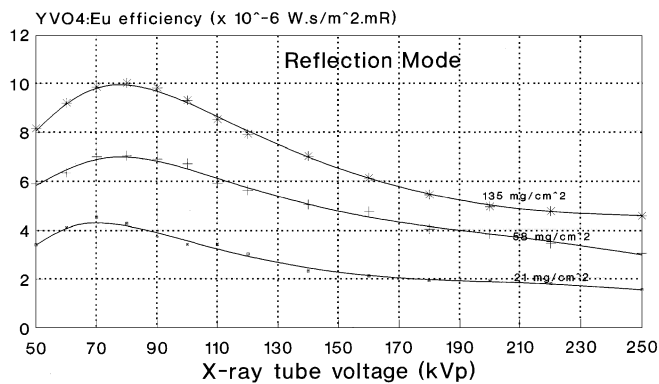


**Fig. 2.** Absolute efficiency of three  $\text{YVO}_4:\text{Eu}$  screens against X-ray tube voltage in reflection mode observation. *Points*: experimental data; *solid lines*: theoretical results

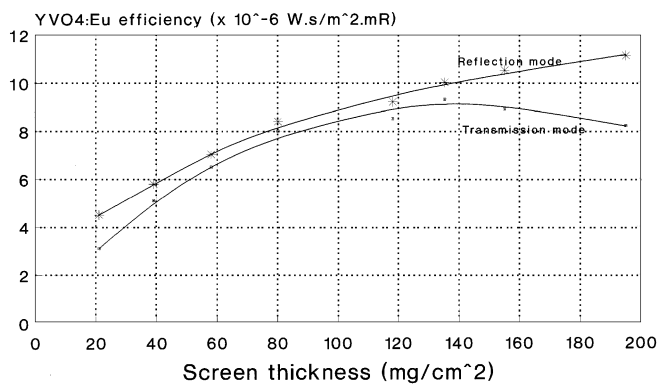


**Fig. 3.** Variation of peak absolute efficiency of  $\text{YVO}_4:\text{Eu}$  screens with coating thickness in transmission and reflection modes. *Points*: experimental data; *solid lines*: theoretical results

photons, created mainly near the front screen surface, have to penetrate before exiting the emitting surface in transmission mode. The Hamaker-Ludwig formulas (appendix) also predict higher values for  $n_R(E)$  relative to  $n_T(E)$ , for the same values of parameters  $\mu$ ,  $\sigma$ ,  $\beta$ ,  $n_c$ . All curves showing the variation of absolute efficiency with tube voltage or screen coating thickness are similar in

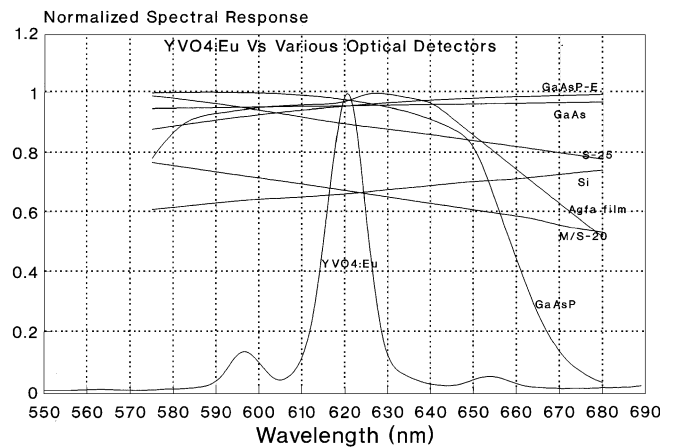


**Fig. 4.** Emitted light spectrum of  $\text{YVO}_4:\text{Eu}$  and spectral sensitivity curves of some common optical photon detectors

shape to the corresponding curves of other fluorescent materials [3, 4]. This particular shape is determined by (a) the quantum efficiency, which describes the X-ray absorption mechanisms within the phosphor material and depends on the coefficient  $\mu$  and the screen coating thickness, (b) the intrinsic X-ray to light conversion efficiency ( $n_c$ ), and (c) the light transmission efficiency within the phosphor material, which depends on the light scattering ( $s$ ) and absorption ( $a$ ) coefficients as well as the screen coating thickness ( $W$ ). Analytical description and prediction of absolute efficiency curves can be found in previous studies [6, 7].

Solid lines in Figs 1–3 represent theoretical results calculated according to the Hamaker-Ludwig model and fitted to experimental data. Intrinsic conversion efficiency  $n_c$  and coefficient  $\sigma$  were estimated by this fitting and found equal to  $n_c = 0.07$  and  $\sigma = 35 \text{ cm}^2/\text{g}$ . Coefficient  $\beta$  was found equal to  $\beta = 0.03$ . Intrinsic conversion efficiency value was close to that reported by Alig and Bloom [12] for cathodoluminescence efficiency ( $n_c = 0.06$ ), lower than  $\text{Y}_2\text{O}_2\text{S}:\text{Eu}$  ( $n_c = 0.11$ ) found by Giakoumakis et al. [4], but higher than the intrinsic efficiency of  $\text{CaWO}_4$  ( $n_c = 0.04$ ) conventionally used in radiography.

The absolute efficiency of  $\text{YVO}_4:\text{Eu}$  screens was lower than that corresponding to other yttrium compound phosphors such as  $\text{Y}_2\text{O}_2\text{S}:\text{Eu}$ , also prepared by sedimentation [4]. This was due to the relatively low value of intrinsic conversion efficiency and the high value of coefficient  $\sigma$ , representing light intensity losses due to absorption and scattering of optical photons within the screen material. These values ( $n_c = 0.07$ ,  $\sigma = 35 \text{ cm}^2/\text{g}$ ) were worse than those of  $\text{Y}_2\text{O}_2\text{S}:\text{Tb}$  ( $n_c = 0.18$ ,  $\sigma = 30 \text{ cm}^2/\text{g}$ ) [3] and  $\text{Y}_2\text{O}_2\text{S}:\text{Eu}$  ( $n_c = 0.11$ ,  $\sigma = 15 \text{ cm}^2/\text{g}$ ) [4]. The low efficiency of  $\text{YVO}_4:\text{Eu}$  may be explained if the fundamental electronic gap of  $\text{YVO}_4:\text{Eu}$  is considered. This gap is inversely proportional to the efficiency as reported by Alig and Bloom [12]; in the case of  $\text{YVO}_4:\text{Eu}$  the fundamental electronic gap is equal to 8.0 eV while for  $\text{Y}_2\text{O}_2\text{S}:\text{Eu}$  is 4.6 eV.

Figure 4 shows the measured light spectrum of  $\text{YVO}_4:\text{Eu}$  together with the spectral sensitivity distributions of various optical detectors. Table 1 shows the

calculated matching factors between  $\text{YVO}_4:\text{Eu}$  and the optical detectors. Spectral matching was found excellent

$$n_T = \frac{n_c \gamma t \mu (1 + \rho) e^{(-\mu W)}}{2(\mu^2 - \sigma^2)} \times \frac{(\mu - \sigma)(1 - \beta) e^{(-\sigma W)} + 2(\sigma + \mu\beta) e^{(\mu W)} - (\mu + \sigma)(1 + \beta) e^{(\sigma W)}}{(1 + \beta)(\rho + \beta) e^{(\sigma W)} - (1 - \beta)(\rho - \beta) e^{(-\sigma W)}} \quad (1)$$

$$n_R = \frac{n_c \gamma \mu e^{(-\mu W)}}{(\mu^2 - \sigma^2)} \times \frac{(\mu - \sigma)(\rho + \beta) e^{(\sigma W)} + 2(\sigma\rho - \mu\beta) e^{(-\mu W)} - (\mu + \sigma)(\rho - \beta) e^{(-\sigma W)}}{(1 + \beta)(\rho + \beta) e^{(\sigma W)} - (1 - \beta)(\rho - \beta) e^{(-\sigma W)}} \quad (2)$$

with the Agfa Scopix LT 2B film, GaAs photocathode, GaAsP and extended sensitivity GaAsP photocells, S-25 photocathode, very good with the modified S-20 and extended sensitivity S-20 photocathodes, and with the Si photodiode. Some of those detectors are used in medical imaging, as in X-ray fluoroscopy, image intensifiers, CT detectors, digital radiography CCD arrays. It could be interesting, in future, to examine the image quality characteristics of  $\text{YVO}_4:\text{Eu}$  coupled to some of those optical detectors. Also, Agfa Scopix LT2B film is used in laser imagers of digital imaging systems, but since the film's matching factor was found to be excellent, it would be interesting to investigate if it could be employed as radiographic film in combination with  $\text{YVO}_4:\text{Eu}$  screens, as well as in  $\text{YVO}_4:\text{Eu}$  containing monitor screens used in multiformat camera imagers.

**Table 1.** Matching factor values between the  $\text{YVO}_4:\text{Eu}$  light spectrum and the spectral sensitivity distributions of various common optical detectors

Optical detectors	Matching factor
Photocathode GaAs	0.955
Photocathode S-25	0.896
Photocathode modified S-20	0.671
Photocathode extended S-20	0.617
Photodiode Si	0.662
Photodiode Ge	0.354
Photocell GaAsP-E	0.953
Photocell GaAsP	0.945
Agfa Scopix film LT 2B	0.956

*Acknowledgement.* This study is dedicated to the memory of late Prof. G.E. Giakoumakis, a leading member of our team, whose work on phosphor materials has inspired us all to continue.

## APPENDIX

Absolute efficiency was calculated employing the theoretical model by Hamaker [7] and Ludwig [6]. This model

predicts the absolute efficiency of a phosphor screen excited by monochromatic X-rays by the following equations:

where  $n_T, n_R$  are the absolute efficiency in transmission and reflection mode, respectively,  $n_c$  is the intrinsic efficiency of the phosphor,  $\mu$  the mass absorption coefficient for the incident X-ray photons,  $W$  the coating thickness (surface density) of the screen,  $t$  the transparency of the screen's substrate,  $\rho = (1 - r)/(1 + r)$ , where  $r$  the reflectivity of the screen's substrate,  $\gamma$  the conversion factor converting the exposure rate (mR/s) to energy fluence of the X-ray beam ( $\text{W}/\text{m}^2$ ), and  $\sigma, \beta$  are the coefficients directly related to the absorption ( $a$ ) and scattering ( $s$ ) coefficients of optical photons within the screen, by  $\sigma = [a(a + 2s)]^{1/2}$  and  $\beta = [a/(a + 2s)]^{1/2}$ .

## References

1. S.P. Wang, O. Laudi, H. Lucks, K.A. Wickersheim, R.A. Buchanan: IEEE Trans. NS-17, 49 (1970)
2. K.A. Wickersheim, R.V. Alves, R.A. Buchanan: IEEE Trans. NS-57 (1970)
3. G.E. Giakoumakis, C.D. Nomicos, E.N. Yiakoumakis, E.K. Evangelou: Phys. Med. Biol. **35**, 1017 (1990)
4. G.E. Giakoumakis, C.D. Nomicos, P. Skountzos, S. Koutroubas, A. Zisos, E.N. Yiakoumakis, M.C. Katsarioti, J.A. Kaliakatsos, M. Rovithi, G.S. Panayiotakis, E.K. Evangelou: Med. Phys. **20**, 79 (1993)
5. K. Matsumoto, T. Kawanishi and K. Takagi: J. Cryst. Growth **55**, 376 (1981)
6. G.W. Ludwig: J. Electrochem. Soc. **118**, 1152 (1971)
7. H. Hamaker: Philips Res. Rep. **2**, 55 (1947)
8. E. Storm: Phys. Rev. A **5**, 2328 (1972)
9. E. Storm, H. Israel: *Photon Cross-Sections from 0.001 to 100 MeV for Elements 1 Through 100*, Report LA-3753 (Los Alamos Scientific Laboratory, University of California, CA 1967)
10. E.B. Saloman, J.H. Hubbell, J.H. Scofield: A. Data Nucl. Data Tables **38**, 1 (1988)
11. G.E. Giakoumakis: Appl. Phys. A **52**, 7 (1991)
12. R.C. Alig, S. Bloom: J. Electrochem. Soc. **124**, 1136 (1977)